To be published in Review of Scientific Instruments, May 1999

Nanoindentation and contact stiffness measurement using force modulation with a capacitive load-displacement transducer.

S.A.Syed Asif*, K.J.Wahl and R.J.Colton
Code 6170, Chemistry Division, Naval Research Laboratory, Washington, DC 20375-5342
**Materials Science and Engineering, University of Florida, Gainesville, FL 32611*

We have implemented a force modulation technique for nanoindentation using a three-plate capacitive load-displacement transducer. The stiffness sensitivity of the instrument is ~0.1 N/m. We show that the sensitivity of this instrument is sufficient to detect long-range surface forces and to locate the surface of a specimen. The low spring mass (236 mg), spring constant (116 N/m) and damping coefficient (0.008 Ns/m) of the transducer allows measurement of the damping losses for nanoscale contacts. We present the experimental technique, important specimen mounting information, and system calibration for nanomechanical property measurement.

I. Introduction

Studying the mechanical response of materials at the nanoscale has received much attention in recent years. These studies have been motivated by the development of new nanostructured materials and continued miniaturization of engineering and electronic components, thin film technology and surface coatings. Measurement of nanoscale mechanical properties of materials is very important in understanding the behavior of asperity contacts in tribology, the initiation of plastic deformation or fracture, and even more surface specific problems such as the role of oxides or adsorbed contaminant layers. Three different techniques and instruments have been developed for these studies: (1) the surface force apparatus (SFA) developed by Israelachvili and Tabor[1]; (2) the atomic force microscope (AFM) developed by Binnig et al.[2] and (3) the depth sensing nanoindentation technique developed by Pethica et al[3]. The capabilities of these instruments cover a wide range of contact area (from several μm^2 in the case of SFA down to a few nm^2 in AFM studies) and displacement resolution. The SFA is mainly used for direct measurements of surface and intermolecular forces and not for surface elastic and plastic properties of materials. While the AFM was used early to investigate elastic and plastic properties at nanoscale[4,5], conventional force detection techniques (inferred from the known spring constant of the lever), small tip size, and unknown tip shape, the contact area is difficult to measure, hence the measured mechanical properties are usually only qualitative. Recent developments in scanning probe microscopy, combining depth sensing nanoindentation with imaging capabilities[6,7] reduces problems in quantifying load-displacement data. Accurate determination of both contact area and displacement can be achieved by coupling depth sensing nanoindentation with force modulation[8], allowing quantitative measurement of nanoscale mechanical properties (hardness, modulus, viscoelasticity, and creep).

In nanoindentation a load is continuously applied to the indenter and the depth of penetration of the indenter (or displacement into the specimen) is measured as a function of load. From the unloading slope of the load-displacement data the contact stiffness, contact area, and mechanical properties such as hardness and modulus of the materials are calculated using well-established models[9]. The force modulation method[8] offers a significant improvement in this technique. In force modulation a small sinusoidal force (AC force) is superimposed on the quasi-static force (DC force) applied to the indenter. The resulting modulation in the displacement (AC displacement amplitude) and the phase shift between the AC force and displacement is measured using a lock-in amplifier. The contact stiffness is calculated from the amplitude and phase shift using a dynamic model [8, 10]. The advantage of force modulation is that the contact stiffness can be directly obtained continuously during indentation. Because measurements are carried out at frequencies greater than 40Hz, it is less sensitive to thermal drift, allowing accurate observation of creep in nanoscale contacts[11]. The technique can also be extended to study the viscoelastic properties of polymeric materials[10] . The ultimate sensitivity and useful frequency range of the technique depend on the mass, the damping coefficient, and stiffness of the indenter. A low mass, low damping coefficient and optimum stiffness of the indenter will significantly improve sensitivity.

In this article we report the development of a force modulation technique using a capacitive load-displacement transducer capable of indenting and imaging. We show that the sensitivity of this instrument is sufficient to detect long-range surface forces and locate the surface of a specimen. We also present practical information on specimen mounting, the dynamic calibration of the instrument, and limitations due to machine compliance.

II. EXPERIMENT AND METHODOLOGY

A. Mechanical configuration of the indenter

The nanoindentation instrument consists of a load-displacement transducer with electrostatic force actuation and displacement sensing electronics (Hysitron Inc., Minneapolis, MN) and an AFM base with piezo scanner, signal access module, and XYZ scanning electronics (Digital Instruments Nanoscope III with "JV" AS-130V scanner, Santa Barbara,

Report Documentation Page

Form Approved
OMB No. 0704-0188

1. REPORT DATE	2. REPORT TYPE	3. DATES COVERED
MAY 1999		**00-00-1999 to 00-00-1999**

4. TITLE AND SUBTITLE	5a. CONTRACT NUMBER
Nanoindentation and contact stiffness measurement using force modulation with a capacitive load-displacement transducer	5b. GRANT NUMBER
	5c. PROGRAM ELEMENT NUMBER
6. AUTHOR(S)	5d. PROJECT NUMBER
	5e. TASK NUMBER
	5f. WORK UNIT NUMBER
7. PERFORMING ORGANIZATION NAME(S) AND ADDRESS(ES) **Naval Research Laboratory,Code 6170,4555 Overlook Avenue, SW,Washington,DC,20375**	8. PERFORMING ORGANIZATION REPORT NUMBER
9. SPONSORING/MONITORING AGENCY NAME(S) AND ADDRESS(ES)	10. SPONSOR/MONITOR'S ACRONYM(S)
	11. SPONSOR/MONITOR'S REPORT NUMBER(S)

12. DISTRIBUTION/AVAILABILITY STATEMENT
Approved for public release; distribution unlimited

13. SUPPLEMENTARY NOTES

14. ABSTRACT

15. SUBJECT TERMS

16. SECURITY CLASSIFICATION OF:			17. LIMITATION OF ABSTRACT	18. NUMBER OF PAGES	19a. NAME OF RESPONSIBLE PERSON
a. REPORT **unclassified**	b. ABSTRACT **unclassified**	c. THIS PAGE **unclassified**		**6**	

CA). The transducer assembly sits atop the AFM base replacing the AFM head. The specimen is mounted on the piezo scanner. The experimental set-up is shown in Fig.1. The load-displacement transducer consists of a three parallel plate (Be-Cu) capacitive structure to apply a force via electrostatic actuation and sense displacement by monitoring the change in capacitance. A Berkovich diamond indenter tip is screwed into the tip holder on the center plate, which is spring mounted to the housing. The outer drive plates are fixed and the center plate and indenter can move in the space between the two drive plates.

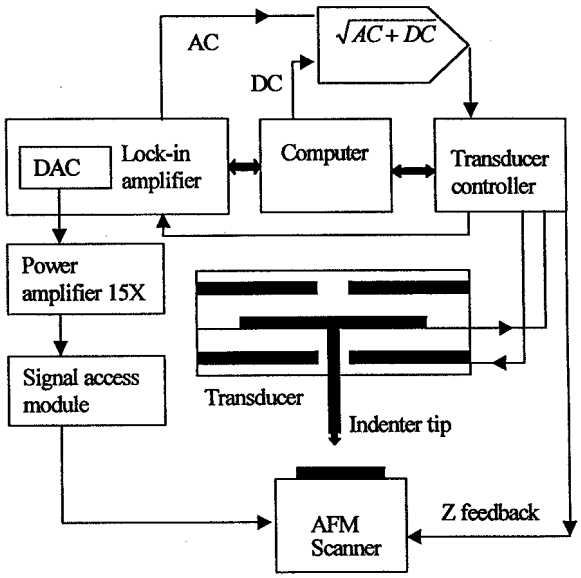

FIG. 1. Schematic diagram of the experimental apparatus.

To apply a load, a voltage, V, is applied between the center plate and bottom plate. This generates an electrostatic force, F,

$$F = E_f V^2 \tag{1}$$

where E_f is the electrostatic force constant which is dependent on the area, A, of the plates and the spacing, d, between the center and outer plates.

$$E_f \sim \frac{A}{d^2} \tag{2}$$

The variation of E_f for this transducer is less than 2% for displacements less than 800 nm. The load resolution is ~100 nN. Vertical displacement of the tip is determined by measuring the displacement of the center plate relative to the two outer plates using the change in capacitance; displacement resolution is ~0.1 nm.

The above configuration allows both indentation and imaging of the specimen before and/or after indentation. The piezo scanner has a lateral (X,Y) scan range of 125x125μm^2 and vertical (Z) range of 5 μm. Vertical movement of the scanner is used for fine approach of the specimen towards the indenter tip. The vertical displacement of the scanner was calibrated using the capacitive displacement transducer. Indentation experiments are performed using either the transducer head to generate the indent with force control or by ramping the specimen toward and away from the indenter using the scanner with displacement control. A computer with a data acquisition board (PCI-MIO-16XE-10, National Instruments, Austin, TX) and software (Labview, National Instruments, Austin, TX) is used to control the indenter head and scanner motion as well as collect data. A DSP two-channel lock-in amplifier (SR830, Stanford Research Systems, Sunnyvale, CA) controlled through a GPIB card (AT-GBIB/TNT, National Instruments, Austin, TX) is used to detect signals during the modulation experiments as well as provide the 16-bit digital-to-analog converters (DACs) (±10 V) for controlling the scanner motion. The DAC output voltage levels are amplified 15X to drive the scanner in the X, Y and Z directions. The software was programmed to allow both simple XY displacements of the specimen to locate an indentation region as well as to perform an array of indents. Imaging is accomplished by combining displacement feedback from the indenter transducer with the AFM scanning electronics and is controlled using the AFM software. For constant rate loading and unloading indentation experiments the data acquisition board was programmed to give voltage output according to equation 1.

B. Force modulation

For force modulation, a small sinusoidal AC force is superimposed on the DC applied load. This is achieved by summing the DC and AC voltage, which is applied to the drive plates. Note that the electrostatic force generated is proportional to the square of the applied voltage (Eqn.1); therefore to achieve a linear load ramp superimposed with pure sinusoidal force modulation the voltage signal was processed electronically using an AD534JN (Analog devices) analog multiplier as a square rooter as shown in Fig. 1. The resulting oscillation in displacement is monitored using the two-channel lock-in amplifier.

For a superimposed driving force $F = F_0 \sin wt$, the equation of motion of the indenter relative to the indenter head is then

$$m\ddot{x} + C\dot{x} + kx = F_0 \sin wt \tag{3}$$

The solution to the above equation is a steady-state displacement oscillation at the same frequency as the excitation

$$x = X \sin(wt - f) \tag{4}$$

where X is the amplitude of the displacement oscillation and f is the phase shift of the displacement with respect to the exciting force.

The amplitude and phase shift can be used to calculate the contact stiffness using a dynamic model[8]. The indenter and contact are represented by the components in the dynamic model as shown in Fig. 2. The standard analytical solution for this model, assuming that the machine frame stiffness K_m is infinite, follows.

The amplitude of the displacement signal is

$$X_o = \frac{F_o}{\sqrt{\left(k - mw^2\right)^2 + \left((C_i + C_s)w\right)^2}} \quad (5)$$

and the phase shift between force and displacement is

$$f = \tan^{-1}\frac{(C_i + C_s)w}{k - mw^2} \quad (6)$$

where F_o is the AC force amplitude, m is the indenter mass, w is the frequency in radians/s, C_i is the damping coefficient of the air gap in the capacitive displacement sensor, and C_s is the damping coefficient of the specimen. The combined stiffness, *k*, is given by

$$k = K_s + K_i \quad (7)$$

where K_s is the contact stiffness and K_i is the spring constant of the leaf springs that hold the indenter shaft.

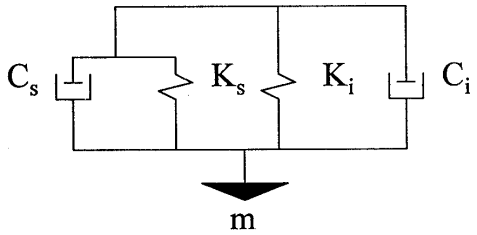

FIG. 2. Dynamic model of indenter system in contact with specimen, where *m* is the indenter mass, C_i is the damping coefficient of the air gap in the capacitive displacement sensor, C_s is the damping coefficient of the specimen, K_s is the contact stiffness and K_i is the spring constant of the leaf springs that hold the indenter shaft.

The indenter spring constant was obtained by applying the DC force and measuring the DC displacement when the indenter tip is free of contact with the specimen surface. Once the spring constant is known, the mass of the indenter can then be determined by measuring the zero load displacement of the transducer. The displacement amplitude X_o and the phase shift f are directly obtained from the DSP lock-in amplifier. When the indenter is not in contact with the specimen surface, that is for a freely suspended indenter, the damping coefficient of the air gap C_i can be obtained by substituting the values of the known constants and the measured displacement amplitude X_o into Eqn.5. If all these constants are known or accurately calibrated then the contact stiffness K_s can be calculated using Eqn.5-7. In an indentation experiment the contact stiffness is proportional to the contact area, *A*[9],

$$K_s = 2E^*\sqrt{\frac{A}{p}} = 2E^* h\sqrt{\frac{24.5}{p}} \quad (8)$$

where 24.5 is a geometric factor arising from the tip shape (Berkovich indenter), E^* is the reduced modulus[12] and *h* is the depth of penetration. If the modulus of the material is known then the contact area can be calculated using the stiffness equation and the hardness can be measured.

$$H = \frac{F^{DC}}{pK_s^2}4E^{*2} \quad (9)$$

If the modulus of the material is not known, the contact area can be measured from the load-displacement data with accurate tip shape calibration[9] and the modulus calculated using the measured contact area and contact stiffness.

For materials which can damp the superimposed AC force, $K_s^{'}$ (or the storage component) is the stiffness component in-phase with the applied force, and $K_s^{''} = wC_s$ (or the loss component) is the stiffness component out-of-phase with the applied force. If both components of the stiffness are known then the storage and loss modulus can be obtained from Eqn. 8.

C. Dynamic response and calibration

To study the frequency dependent properties of materials (i.e. loss and storage modulus of polymers) at the nanometer scale it is necessary to know the dynamic response of the indenter system. This is mainly because what is measured is the total response of the experimental system, that is the combined response of the measuring apparatus and specimen. To determine the dynamic response of the indenter system when it is free of contact, the frequency of the AC force was changed from 1-300 Hz. The amplitude and phase shift at each frequency are measured with the lock-in amplifier, and the dynamic compliance (AC displacement / AC force) is calculated for each frequency (Fig. 3a). A model fit was done for the dynamic compliance data with a function of the same form as the dynamic model (Eqn. 5). The fitting parameters

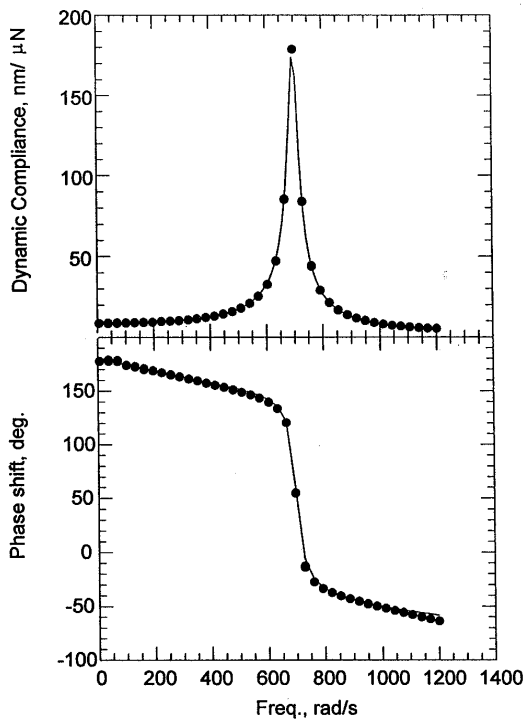

FIG.3a. Dynamic compliance of the freely suspended indenter. The solid line is the model fit. 3b. The phase shift as a function of frequency. The solid line is the model fit.

are m, K_s and C_i. The correlation between the dynamic model and actual dynamic response is excellent (r=0.9999). From the fit, the resonance frequency of the system is 110 Hz, the damping coefficient is 0.008 Ns/m, the mass is 236 mg, and the spring constant is 116 N/m.

Fig.3b shows the phase shift as a function of frequency due to damping of the center plate. The small difference between the model fit and measured phase shift is largely due to the electronics (i.e. low pass filter). If the time constant of the electronics is known, this difference can be eliminated. With accurate calibration of the indenter constants and frequency response of the system, the contact stiffness can be calculated using Eqns. 5-7 and the modulus or hardness of the material can be determined.

D. Contact detection and indentation

One of the problems in nanoindentation is detecting the surface of the specimen (to indent) without any initial contact damage. Normally it is done by monitoring the displacement of the indenter tip as it comes in contact with the specimen; when the displacement reaches a preset value it is assumed that the indenter tip is on the specimen surface. This approach may work well for rigid materials but for compliant materials like polymers or metals (e.g. indium, lead, etc.) it is difficult to find the specimen surface without initial contact damage. However, it is possible to detect the surface with far greater sensitivity before any contact damage using the following procedure.

The indenter-specimen approach is done in two steps: the stepper motor for coarse approach and the Z displacement of the scanner for fine approach. In the first step, the specimen is moved towards the tip using the stepper motor with a set point of 1 μN preset DC load using the AFM control software. After this coarse approach, the scanner is disabled from the feedback control. Then a working distance is set by retracting the scanner from the tip using the Z piezo. The working distance can be set to 0-3000 nm, depending upon the surface roughness of the specimen. The specimen is then moved to a new location using the scanner (XY piezo) for the indentation experiment. The indenter tip is modulated at resonance frequency (110 Hz) with an AC force of 150 nN. The AC displacement and phase shift is monitored using the lock-in amplifier.

In the second step the specimen approaches the indenter tip (fine approach) by ramping the piezo scanner at 1nm/s. As the specimen comes closer to the indenter tip, the tip interacts with the specimen surface via long-range surface forces. This alters the resonance frequency of the tip and induces a phase shift in the displacement signal. The phase shift is used to detect the specimen surface. The preset value of the phase shift can be set to a desired value depending upon the specimen. For compliant specimens (i.e. polymer or indium) a 5-degree phase shift is sufficient to detect the surface. Once the phase shift reaches the preset value, the scanner ramp is stopped and the indenter tip displacement is monitored for thermal drift. The indentation experiments are carried out only when the thermal drift is less than 0.05 nm/s.

The above procedure can be used to generate a stiffness curve, similar to a force-displacement curve in AFM experiments[4]. The specimen approaches the indenter tip until the phase shift reaches the preset value. Then the specimen is withdrawn until the phase shift reaches the original value. The AC displacement amplitude and phase shift is directly obtained from the lock-in amplifier during approach and retraction, and the stiffness is calculated using Eqns. 5-7.

The indentation experiments are carried out in a loading and unloading sequence. The indentation experiments can be pre-programmed with as many segments as desired. In each segment the indentation parameters, i.e. loading rate, frequency and amplitude of the AC force, sensitivity and time constant of the lock-in amplifier, can be set individually.

III. RESULTS AND DISCUSSION

A. Stiffness curve

Fig.4a is the approach-retract curve for indium showing the phase shift as a function of displacement. The indenter tip is modulated with an AC force of 150 nN at 110 Hz. The initial phase shift when the tip is away from the specimen surface is ~ 85°. As the specimen comes closer to the tip the phase shift decreases. When the phase shift reaches 80°, i.e. 5°

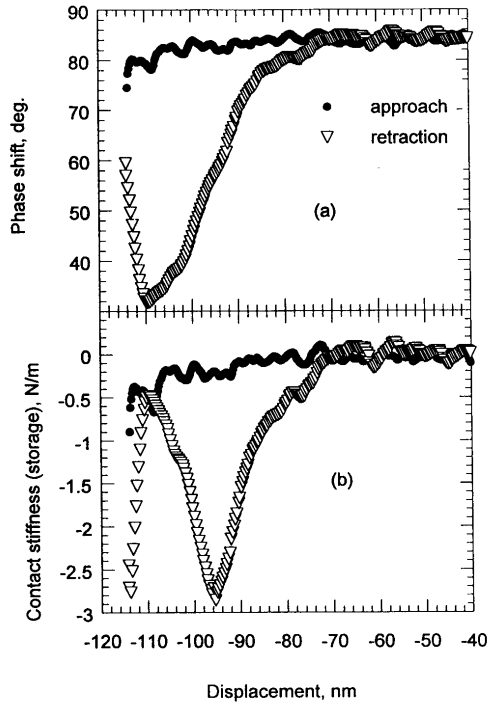

FIG.4a. The phase shift as a function of specimen displacement during approach and retraction for an indium specimen. 4b. The contact stiffness as a function of specimen displacement during approach and retraction for an indium specimen.

shift from the original value, the specimen is withdrawn from the tip. However, it can be seen that the phase continued to decrease to 30° before it recovered to the original value.

Fig.4b shows the variation in contact stiffness due to tip-surface interaction. The contact stiffness is obtained by subtracting the indenter spring constant (116 N/m) from the

total stiffness (Eqn. 7). Zero contact stiffness means there is no interaction between the tip and specimen surface. As the specimen comes closer to the tip the contact stiffness slowly becomes negative and suddenly decreases to a maximum value of -2.8 N/m. The negative stiffness means the tip experiences an attractive force (note that the experiments were conducted in air with a relative humidity of 54%). The observed negative stiffness is probably due to long-range capillary forces. After a 5^o phase shift the specimen is pulled away from the tip at a rate of 1 nm/s. However, it appears from Fig.4a and b that the tip is still pulled towards the specimen surface. The distance between the tip and specimen surface now depends on the relative movement of the tip and specimen. As the specimen comes closer to the tip the repulsive interaction increases the contact stiffness (becomes more positive). When the specimen is pulled further away from the sample the contact stiffness again decreases to -2.9 N/m due to other net attractive forces (i.e. adhesion between tip and specimen) and then recovers to its original zero stiffness. Adhesion and capillary neck formation can be inferred from the stiffness variation during retraction. These results are similar to those of Jarvis et al.[13] using AFM in force modulation mode. They also clearly demonstrate the sensitivity of the force modulation technique and our experimental set-up. The stiffness sensitivity is less than 1 N/m, and it is possible to detect long-range surface forces. The results also indicate that for experiments conducted in air, where the surfaces are likely covered with adsorbed water, shallow indentations (below 20-30nm) will lead to inaccurate results if homogeneous material properties are assumed.

B. Cantilever experiments

To verify that the measured stiffness using the AC force modulation technique is identical to that obtained using the DC load-displacement technique, several experiments were carried out on a cantilever specimen. A special cantilever was prepared from tantalum foil and mounted on a glass substrate using super glue. The indenter tip was brought into contact with the free end of the cantilever and the load was ramped at a constant rate to the desired maximum load and then unloaded. A typical load-displacement plot for the cantilever is shown in Fig.5. The cantilever stiffness is measured from the slope of the load-displacement plot and is 580 N/m (r=0.98).

To measure the contact stiffness using the force modulation technique an AC force of 300 nN at 40 Hz was applied during loading and unloading. From the measured phase shift and amplitude of the AC displacement signal it

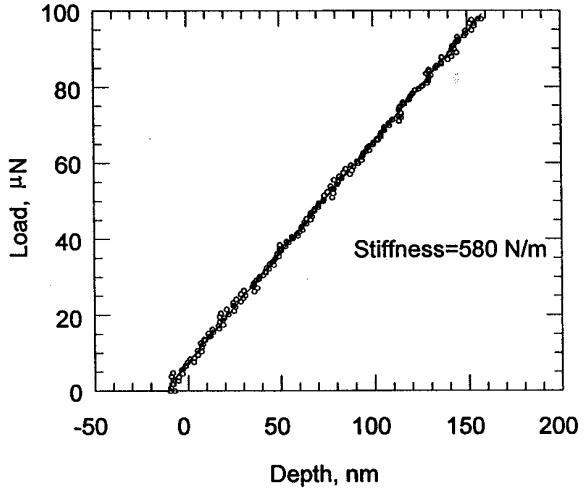

FIG. 5. The load-displacement data for a tantalum cantilever. The slope is the stiffness of the cantilever.

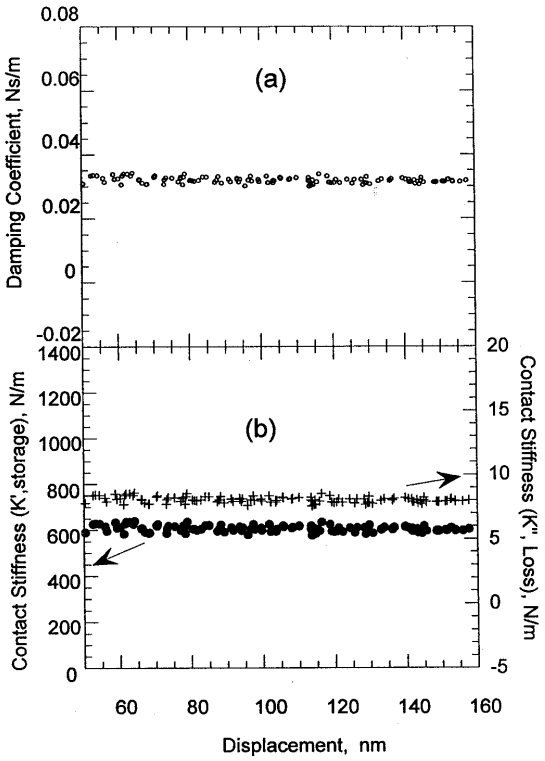

FIG.6a. The damping coefficient of a tantalum cantilever glued on to a glass substrate at one end showing some damping loss due to the glue. 6b. The stiffness of a tantalum cantilever glued on to a glass substrate showing storage and loss component due to damping.

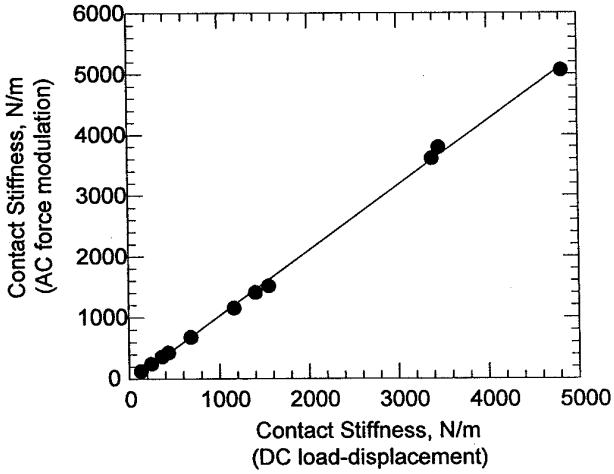

FIG.7. Comparison of cantilever stiffness measurement using DC load-displacement method and AC force modulation method at 40 Hz.

was found that the cantilever specimen, which was supposed to respond like an ideal spring, was actually damped. Fig.6a shows the damping coefficient as a function of displacement for the cantilever specimen using Eqn.6. The main source of damping was likely the glue used to mount the cantilever to the glass substrate. Fig.6b shows the storage and loss component of the cantilever stiffness as a function of displacement. The storage component of the stiffness, 600±10 N/m, is in good agreement with the stiffness measured using the DC technique. The loss component of the stiffness is 8±1 N/m. This experiment demonstrates the importance of specimen mounting in nanoindentation experiments. If the specimens are not mounted rigidly, there may be a loss of energy, which may influence the mechanical response of the specimen.

Similar experiments were carried out at different locations along the length of the cantilever. One limitation of the dynamic model (Fig.2) is the assumption that the machine stiffness is infinite. This assumption is valid only if the contact stiffness is at least 2-3 orders of magnitude less than the machine stiffness. The machine stiffness for the present experimental setup is 10^5 N/m. Therefore the maximum contact stiffness that can be measured reliably is of the order of 10^3 N/m. Fig.7 shows the comparison between the stiffness measured using the DC load-displacement technique and the AC force modulation technique. It can be seen that a good correlation exists between the AC and DC technique.

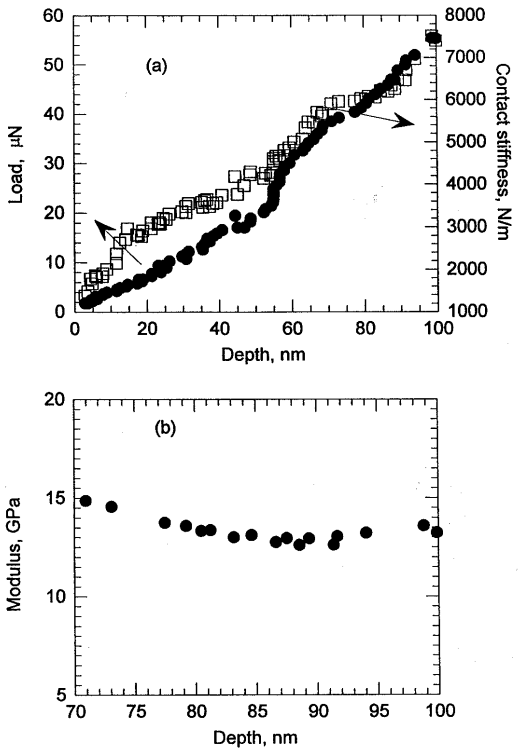

FIG.8a. The load-displacement and contact stiffness data for an indium specimen. 8b. The Young's modulus as a function of depth for an indium specimen.

C. Indentation experiments

Some indentation experiments were carried out on an electro-polished indium specimen[14]. Fig.8a shows typical indentation load-penetration depth and stiffness-penetration depth curves for indium. Indium is a compliant metal with a modulus of 12-14 GPa[15]. The maximum DC load applied was ~50 μN and the AC force ~1.5 μN at 40 Hz. It can be seen that the contact stiffness increased with indentation depth. From the measured depth and contact stiffness the modulus of the material was calculated from Eqn. 8. To avoid tip shape and surface contamination artifacts, only the data for indentation depths ranging from ~70-100 nm were used to calculate the modulus. Fig. 8b shows the modulus as a function of depth for indium specimens. The measured modulus (13.1 ± 1 GPa) is in reasonable agreement with the bulk value.

ACKNOWLEDGMENTS

The authors thank Hysitron, Inc. and Ken Lee for help and assistance with the instrument development. S.A.S.Asif thanks the University of Florida for funding through a DOD/AFOSR MURI Post Doctoral Fellowship. This work was supported in part by the Office of Naval Research.

REFERENCES

[1] J.N. Israelachvili and D. Tabor, Proc. R. Soc. London A **331**,19 (1972).
[2] G. Binnig, C.F. Quate, and CH. Gerber, Phys. Rev. Lett. **56**, 930 (1986).
[3] J.B. Pethica, R. Hutchings and W.C. Oliver, Phil.Mag. A **48**, 593, (1983).
[4] N.A. Burnham and R.J. Colton, J.Vac.Sci. Technol. A **7**, 2906 (1989).
[5] N.A. Burnham, R.J. Colton and H.M. Pollock, Nanotechnology **4**, 64 (1993).
[6] A.J. Stephen and J.E. Houston, Rev. Sci. Instrum, **62**, 710, (1990).
[7] B. Bhushan, A.V. Kulkarni, W. Bonin, J.T. Wyrobek, Phil. Mag. A. 74, 1117 (1996).
[8] J.B. Pethica and W.C. Oliver, Phys. Scr. T **19**, 61 (1987).
[9] W.C. Oliver and G.M. Pharr, J.Mater. Res, **7**, 1564 (1992).
[10] S.A. Syed Asif, D.Phil Thesis, Oxford University (1997).
[11] S.A. Syed Asif and J.B. Pethica, Phil. Mag. A **76**,1105 (1997).
[12] K.L. Johnson, Contact Mechanics, Cambridge University Press, 92 (1985).
[13] S.P. Jarvis. A. Oral, T.P. Weihs and J.B. Pethica, Rev. Sci. Instrum. **64**,12 (1993).
[14] E.A. Brandes, Smithells Metal Reference Book, London, **6**,10 (1983).
[15] S.A. Syed Asif and J.B. Pethica, Journal of Adhesion, **67**,153 (1998).